

Nonsequential double ionization with few-cycle laser pulses

X. Liu

*Max-Born-Institut für nichtlineare Optik und Kurzzeitspektroskopie,
Max-Born-Str. 2A, D-12489 Berlin, Germany*

C. Figueira de Morisson Faria

*Institut für theoretische Physik, Universität Hannover, Appelstr. 2, 30167 Hannover
(Dated: July 2, 2018)*

We investigate differential electron momentum distributions in non-sequential double ionization (NSDI) with linearly polarized, few-cycle pulses, using a classical model based on a laser-assisted inelastic (e^- , $2e^-$) rescattering mechanism. We show that these yields, as functions of the momentum components parallel to the laser polarization, are highly asymmetric and strongly influenced by the absolute phase, i.e., the phase difference between the carrier oscillation of a few-cycle pulse and its envelope. Indeed, around a critical phase, such distributions change their sign in a radical fashion. This phase dependence provides a possibility for absolute-phase measurements which is, in principle, superior to the schemes involving high-order harmonic generation or above-threshold ionization.

Recently, few-cycle laser pulses of intensities around or higher than $10^{14}\text{W}/\text{cm}^2$ have proven to be extremely important. A particular characteristic of such pulses is that they may have very high intensities and, still, carry much less energy than their longer counterparts, such that, effectively, ionization is reduced. This has extended the damage threshold of solid-state materials up to the intensities in question [1], and has made the generation of high-order harmonic radiation up to astonishingly high frequencies possible [2]. Furthermore, their length, of the order of a few fs , permits controlling processes such as molecular motion or chemical reactions [3], as well as the production of isolated, X-ray attosecond pulses [4].

In this pulse-length regime, the so-called “absolute phase”, i.e., the phase difference between the envelope of the pulse and its carrier frequency, has considerable influence on several strong-field phenomena, as for instance high-order harmonic generation (HHG) [5] and above-threshold ionization [6] (ATI) [7, 8]. Indeed, this phase determines features such as the maximal harmonic or photoelectron energy, the time profile of both phenomena, and the intensity of the ATI or HHG yields.

This is not surprising, since the physics of HHG and ATI is directly related to the *instantaneous*, time dependent field. HHG, for instance, is described by a three-step mechanism in which an electron leaves an atom at an instant t_0 through tunneling ionization, propagates in the continuum under the influence of the external laser field and, at a later time t_1 , recombines with a bound state of the parent ion, generating harmonics [9]. Slightly different processes, either in which elastic rescattering with the parent ion is taken as the third step, or in which the electron reaches the detector without recolliding explain the high-order and low-order ATI peaks, respectively [10].

In order to interpret the experimental data obtained in such cases, the precise knowledge of the absolute phase ϕ is required. This poses a serious practical problem, since this phase is difficult to stabilize, to control or to measure [11]. For this reason, schemes for measuring ϕ have been suggested and realized, as, for instance, using

the asymmetry in ATI photoelectron counts [7].

In this Letter, we propose laser-assisted nonsequential double ionization (NSDI) as a tool for absolute phase diagnosis. This phenomenon is being the subject of very active discussion, which was triggered by differential measurements of electron momentum distributions performed with the COLTRIMS (Cold Target Recoil Ion Momentum Spectroscopy) technique, for linearly polarized fields of intensities of the order of $I \sim 10^{14} - 10^{15}\text{W}/\text{cm}^2$ incident in rare-gas samples [12]. Such measurements revealed very peculiar features, namely two symmetric peaks at $p_{1\parallel} = p_{2\parallel} = \pm 2\sqrt{U_p}$, in the $(p_{1\parallel}, p_{2\parallel})$ plane, where $p_{j\parallel}$ ($j = 1, 2$) and U_p denote the momentum components parallel to the laser field polarization and the ponderomotive energy [13], respectively.

These features are explained by a physical mechanism very similar to those in HHG and high-order ATI. The main difference lies on the rescattering process at t_1 , which is now inelastic: the first electron gives part of its kinetic energy upon return to the second electron, so that it can overcome the ionization potential of the singly ionized atom and reach the continuum [9].

This laser-assisted rescattering process has been considered by several groups, using either classical [14], semiclassical [15, 16, 17, 18] or quantum-mechanical [19, 20, 21] approaches, different types of electron-electron interaction [15, 17, 18], and neglecting or including electron-electron repulsion in the final states [17, 18, 19]. So far, since the pulses involved were relatively long, they have been mostly approximated by monochromatic fields.

Particularly what classical models concern, it is astonishing how well they reproduce the main features either observed experimentally, or obtained by means of more refined, quantum mechanical methods. Indeed, recently, we have computed NSDI yields considering rescattering in its simplest form, i.e., electron-impact ionization, both classically and within a quantum-mechanical S-Matrix framework, with practically identical results [17, 18].

In this work, we use a similar classical model as in [17, 18], in which an electron ensemble is subject to a

few-cycle pulse $E(t) = -dA(t)/dt$. The vector potential is given by

$$\mathbf{A}(t) = A_0 \sin^2(\Omega t/2) \sin(\omega t + \phi) \hat{e}_x, \quad (1)$$

with frequency ω , amplitude A_0 , absolute phase ϕ , and $\Omega = \omega/n$, where n denotes the number of cycles. The electrons are ejected in the continuum at a time t_0 with vanishing drift velocities and from the origin of the coordinate system. The start times are uniformly distributed and the ejection probability per unit time, unless stated otherwise, is given by the quasi-static [22] tunneling rate

$$R(t_0) \sim \frac{1}{|E(t_0)|} \exp \left[\frac{-2(2|E_{01}|)^{3/2}}{3|E(t_0)|} \right], \quad (2)$$

where $|E_{01}|$ is the ionization potential of the atom in question. Subsequently, these electrons propagate under the influence of only the laser field. Finally, some of them return to the site of their release and free a second ensemble of electrons through inelastic collisions at a later instant t_1 .

The equations of motion of each pair in such electron ensembles, in atomic units, read

$$[\mathbf{k} + \mathbf{A}(t_0)]^2 = 0, \quad (3)$$

$$\int_{t_0}^{t_1} [\mathbf{k} + \mathbf{A}(t)]^2 dt = 0 \quad (4)$$

and

$$\sum_{j=1}^2 [\mathbf{p}_j + \mathbf{A}(t_1)]^2 = [\mathbf{k} + \mathbf{A}(t_1)]^2 - 2|E_{02}|. \quad (5)$$

Eq. (3) gives the energy conservation at the ionization time. Eq. (4) imposes restrictions upon the intermediate electron momentum \mathbf{k} such that the electron returns to its parent ion. Finally, the third expression (Eq. (5)) yields the energy conservation at the recollision time t_1 . Thereby, the first electron gives part of its kinetic energy $E_{\text{ret}}(t_1) = [\mathbf{k} + \mathbf{A}(t_1)]^2/2$ upon return to the second electron, so that it is able to overcome the ionization potential $|E_{02}|$ of the singly ionized atom. In terms of the momentum components parallel and perpendicular to the electric-field polarization, denoted $p_{j\parallel}$ and $\mathbf{p}_{j\perp}$, respectively, Eq. (5) is written as

$$\sum_{j=1}^2 [p_{j\parallel} + A(t_1)]^2 = [\mathbf{k} + \mathbf{A}(t_1)]^2 - 2|E_{02}| - \sum_{j=1}^2 \mathbf{p}_{j\perp}^2. \quad (6)$$

Eq. (6) describes a circle in the $(p_{1\parallel}, p_{2\parallel})$ plane, centered at $A(t_1)$ and whose radius depends on E_{ret} , $|E_{02}|$ and on $\mathbf{p}_{j\perp}^2$ ($j = 1, 2$). The transverse momenta effectively shift the binding energy which must be overcome such that, depending on this quantity, there are situations for which the rescattering process is classically forbidden.

The electron momentum distributions then read

$$\Gamma \sim \int dt_0 R(t_0) \delta \left(E_{\text{ret}}(t_1) - \sum_{j=1}^2 \frac{(\mathbf{p}_j + \mathbf{A}(t_1))^2}{2} - |E_{02}| \right), \quad (7)$$

where the argument of the δ function gives the energy conservation upon return. The transverse momenta are integrated over. Details about this model are given in [18].

These distributions are displayed in the upper panels of Fig. 1, for neon [23], as density plots in the $(p_{1\parallel}, p_{2\parallel})$ plane. Their circular shapes and the maxima along $p_{1\parallel} = p_{2\parallel}$ are features also present for monochromatic driving fields [24], and mean, physically, that both electrons are leaving the parent ion most probably with equal parallel momenta. However, the fact that the yields are concentrated in only one quadrant of the $(p_{1\parallel}, p_{2\parallel})$ plane, makes them strikingly different from the former distributions, which are symmetric in $(p_{1\parallel}, p_{2\parallel}) \leftrightarrow (-p_{1\parallel}, -p_{2\parallel})$. Furthermore, for a narrow phase interval around a critical phase ϕ_c (c.f. panel (c)), the sign of the momenta $p_{j\parallel}$ change in a rather radical fashion, and the whole yield is shifted from the first to the third quadrant. For increasing pulse length, these effects get less pronounced and practically disappear (Figs. 1(e)–1(h)). The distributions then become symmetric and phase-independent.

Important questions concern the physical origin of both the asymmetry and the critical phase: are they caused by the phase space or by the tunneling rate (2)? Depending on the parameters, a whole phase-space region may become classically inaccessible, such that the radius of the circle described by Eq. (6) would collapse and the corresponding NSDI yields would vanish. The quasi-static tunneling rate, on the other hand, favors the start times t_0 for which the instantaneous field amplitude $|E(t_0)|$ is large, as compared to those for which $|E(t_0)|$ is small. Thus, the contributions to the yield from the former or from the latter case would be enhanced or suppressed, respectively.

In order to single out the influence of the phase space, we assume that the electrons belonging to the first ensemble reach the continuum at a constant rate. Such results are shown in panels (i)–(l) of Fig. 1, and are radically different from those obtained with the more realistic, quasi-static tunneling rate. Indeed, the momentum distributions, though asymmetric, exhibit peaks in *both* first and third quadrants of the $(p_{1\parallel}, p_{2\parallel})$ plane, vaguely resembling those obtained with monochromatic driving fields. The asymmetry is expected, since, for such pulses, the relation $A(t) = -A(t \pm T/2)$, and thus $|\Gamma(t_1, t_0, p_{1\parallel}, p_{2\parallel})| = |\Gamma(t_1 \pm T/2, t_0 \pm T/2, -p_{1\parallel}, -p_{2\parallel})|$, where $T = 2\pi/\omega$, which was true for monochromatic fields, no longer holds. However, the huge effects observed in the upper panels are absent. Physically, this means that there is a momentum region for which the rescattering process is classically allowed but for which the probability that the first electron reaches the continuum is very small. Consequently, even if this region is

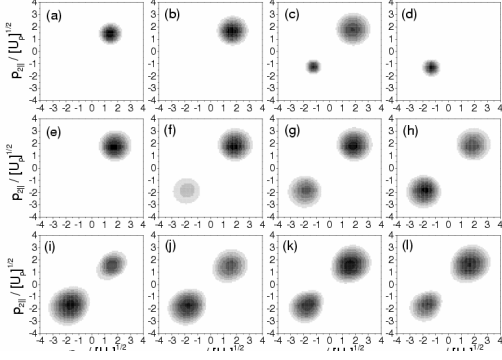


FIG. 1: Electron momentum distributions along the laser polarization, for neon ($|E_{01}| = 0.79$ a.u. and $|E_{02}| = 1.51$ a.u.), subject to pulses of intensity $I = 4.7 \times 10^{14} \text{ W/cm}^2$ and carrier frequency $\omega = 0.057$ a.u., respectively. In panels (a) to (d) and (i) to (l) we consider a four-cycle pulse ($n = 4$), whereas in panels (e) to (h) the pulse length is varied. Panels (a) to (h) and (i) to (l) were computed with the quasi-static and a constant tunneling rate, respectively. Panels (a) and (i): $\phi = 0.1\pi$; panels (b) and (j): $\phi = 0.5\pi$; panels (c) and (k): $\phi = 0.8\pi$; panels (d) and (l): $\phi = 0.9\pi$. In panels (e), (f), and (g) $n = 8$, $n = 12$ and $n = 16$ respectively, and $\phi = 0.1\pi$. In panel (h), n is the same as in (g) and $\phi = 0.9\pi$.

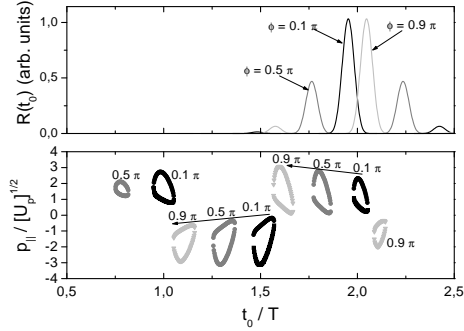


FIG. 2: Parallel electron momenta p_{\parallel} along $p_{1\parallel} = p_{2\parallel}$, for transverse momenta $\mathbf{p}_{\perp} = \mathbf{p}_{2\perp} = 0$, as functions of the start times t_0 of the electrons belonging to the first ensemble, together with the quasi-static tunneling rates. The remaining parameters are the same as in panels (a)–(d) of Fig. 1. The times t_0 are given in units of the field cycle.

large, its contributions to the yield will be negligible.

In Fig. 2 we analyze this effect in detail. Therein, the electron start times t_0 are plotted, together with the quasi-static rate. We restrict the parameter range so that the classically allowed region is most extensive [25], taking parallel momenta along the diagonal $p_{1\parallel} = p_{2\parallel} = p_{\parallel}$ and vanishing transverse momenta [16]. We consider only pairs (t_1, t_0) of start and return times for the first electron such that its excursion time $\Delta t = t_1 - t_0$ in the continuum is of the order of $T/2$ [26]. For the specific parameters of the figure, there exist mainly two sets of electrons for

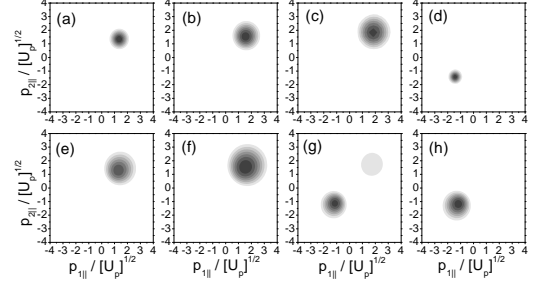


FIG. 3: Parallel electron momentum distributions for pulses of intensities $I = 4 \times 10^{14} \text{ W/cm}^2$ and $I = 8 \times 10^{14} \text{ W/cm}^2$ (upper and lower panels, respectively). The electrons were ejected with the quasi-static tunneling rate. The remaining parameters are the same as in panels (a)–(d) of Fig. 1.

which the quasi-static rate is large and, therefore, whose contributions are relevant: those ejected at $1.5T < t_0 < 2T$, with positive momenta, and those released at $2T < t_0 < 2.5T$, with negative momenta [27].

For a large range of absolute phases $\phi < \phi_c$, electron-impact ionization from the latter set of trajectories is classically forbidden. Thus, the distributions concentrate on the first quadrant. Around the critical phase, this process is allowed for both sets of electrons and the tunneling rates are comparable. Consequently, there are relevant contributions to the yield in the first and third quadrants. This changes for larger phases, as for instance $\phi = 0.9\pi$. In this case, the electrons ejected at $2T < t_0 < 2.5T$ are favored and $p_{j\parallel}$ are mainly negative.

The role of the phase space is even more evident as the driving-field intensity is varied, as shown in Fig. 3. By doing so, one is changing the radius of the circle described by Eq. (6), and thus the region in the $(p_{1\parallel}, p_{2\parallel})$ plane for which rescattering is classically allowed. Therefore, the critical phase may change.

For a lower intensity than that in Fig. 1, the yield in the negative momentum region appears for a phase larger than $\phi_c = 0.8\pi$ (c.f. panels (c) and (d)). This is due to the fact that the classically allowed region for $p_{\parallel} < 0$ is almost vanishing. Thus, even if the tunneling rates are comparable, the first electron, upon return, no longer possesses enough kinetic energy to release the second electron in a way that both leave with negative parallel momenta. For a higher intensity, apart from the fact that both regions are classically allowed, the probability that the second electron is released with negative parallel momentum is larger. Therefore, the transition occurs where expected, as displayed in panel (g). This is confirmed by Fig. 4, where, as the intensity decreases, the dominant set of ionization times ($2T < t_0 < 2.5T$), corresponding to $p_{\parallel} < 0$, collapses.

In conclusion, we perform a theoretical investigation of NSDI with few-cycle pulses, using a classical model

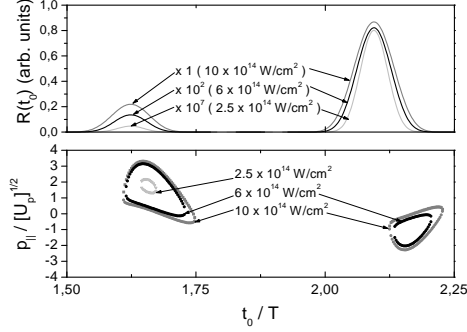


FIG. 4: Parallel electron momenta p_{\parallel} along $p_{1\parallel} = p_{2\parallel}$ and for vanishing transverse momenta, as functions of the start times t_0 , together with the quasi-static tunneling rates, for several driving-field intensities and the critical phase $\phi = 0.8\pi$. The remaining parameters are the same as in Fig. 3. For the lowest intensity, rescattering caused by electrons ejected at $2T < t_0 < 2.5T$ is classically forbidden, so that the corresponding curve is not displayed.

based on electron impact ionization. Both electrons have equal final momentum components parallel to the field polarization, which are mainly positive or negative. The sign of such momenta and their most probable values depend on the absolute phase ϕ . In particular, around a critical phase, these momenta change sign. Such features are explained as the interplay between the tunneling rate for the first electron and the phase space.

The changes in the NSDI yields upon a critical phase are far more extreme effects than those observed for HHG or ATI. In fact, nonsequential double ionization has an advantage over the other two phenomena: the phase space region contributing to the process is *confined*. Thus, for particular ranges of ϕ , it is easier to make a whole region either classically forbidden, by making the radius in Eq. (6) collapse, or irrelevant, by reducing the corresponding ionization rate. Therefore, NSDI is, in principle, a tool for absolute phase diagnosis which is more efficient than the existing schemes.

We thank A. Fring for useful discussions. This work was financed in part by the Deutsche Forschungsgemeinschaft.

-
- [1] M. Lenzner, *et al*, Phys. Rev. Lett. **80**, 4076 (1998).
 - [2] T. Brabec and F. Krausz, Rev. Mod. Phys. **72**, 545 (2000).
 - [3] M. Schnürer, *et al*, Phys. Rev. Lett. **85**, 3392 (2000); M. Hentschel *et al*, Nature **414**, 509 (2001); Niikura *et al*, Nature **417**, 917 (2002); A. Baltuska *et al*, Nature **421**, 611 (2003).
 - [4] M. Drescher, *et al*, Science **291**, 1293 (2001); P.M. Paul, *et al*, Science **292**, 1689 (2001); M. Kitzler, *et al*, Phys. Rev. Lett. **88**, 173904 (2002).
 - [5] A. de Bohan, *et al*, Phys. Rev. Lett. **81**, 1837 (1998)
 - [6] in ATI, an atom absorbs more photons than it is necessary for it to ionize, releasing high-energy electrons.
 - [7] P. Dietrich, *et al*, Opt. Lett. **25**, 16 (2000); G.G. Paulus, *et al*, Nature **414**, 182 (2001); D. B. Milošević, *et al*, Phys. Rev. Lett. **89**, 153001 (2002); S. Chelkowski and A. D. Bandrauk, Phys. Rev. A **65**, 061802 (2002).
 - [8] D. B. Milošević, *et al*, Opt. Express **11**, 1418 (2003).
 - [9] P.B. Corkum, Phys. Rev. Lett. **71**, 1994 (1993); M. Lewenstein, *et al*, Phys. Rev. A **49**, 2117 (1994).
 - [10] G.G. Paulus, *et al*, J. Phys. B **27**, L703 (1994).
 - [11] A. Apolonski, *et al*, Phys. Rev. Lett. **85**, 740 (2000); A. Baltuska, *et al*, Phys. Rev. Lett. **88**, 133901 (2002).
 - [12] R. Moshhammer, *et al*, Phys. Rev. Lett. **84**, 447 (2000); B. Feuerstein, *et al*, Phys. Rev. Lett. **87**, 043003 (2001); T. Weber *et al*, Phys. Rev. Lett. **84**, 443 (2000); Nature **404**, 608 (2000).
 - [13] The ponderomotive energy is the temporal average $U_p = \langle A(t)^2 \rangle_t / 2$, where $A(t)$ is the vector potential. In order to compare our results more directly with the existing literature, we approximate it by the expression for the monochromatic case, i.e., $U_p = 4A_0^2$.
 - [14] J. Chen, *et al*, Phys. Rev. A **63**, 011404 (R) (2000); L.B. Fu, *et al*, *ibid.* **63**, 043416 (2001); Phys. Rev. A **65**, 021406 (R) (2002); *ibid.* **66**, 043410 (2002); R. Panfili, *et al*, Phys. Rev. Lett. **89**, 113001 (2002); S.L. Haan, *et al*, Phys. Rev. A **66**, 061402(R) (2002).
 - [15] S. P. Goreslavskii, *et al*, Phys. Rev. A **64**, 053402 (2002); S.V. Popruzhenko, *et al*, Phys. Rev. Lett. **89**, 023001 (2002).
 - [16] C. Figueira de Morisson Faria and W. Becker, Laser Phys. **13**, 1196 (2003).
 - [17] C. Figueira de Morisson Faria, *et al*, physics/0306143 (2003)
 - [18] C. Figueira de Morisson Faria, *et al*, in preparation (2003)
 - [19] A. Becker and F.H.M. Faisal. Phys. Rev. A **50**, 3256 (1994); M. Weckenbrock, *et al*, Phys. Rev. Lett. **91**, 123004 (2003).
 - [20] R. Kopold, *et al*, Phys. Rev. Lett. **85**, 3781 (2000).
 - [21] J.B. Watson, *et al*, Phys. Rev. Lett. **78**, 1884 (1997); D. Dundas, *et al*, J. Phys. B **32**, L231 (1999); W.C. Liu, *et al*, Phys. Rev. Lett. **83**, 520 (1999); C. Szymanowski, *et al*, Phys. Rev. A **61**, 055401 (2000); M. Lein, *et al*, Phys. Rev. Lett. **85**, 4707 (2000).
 - [22] L.V. Keldysh, Zh. Éksp. Teor. Fiz. **47**, 1945 (1964) [Sov. Phys. JETP **20**, 1307 (1965)]
 - [23] For neon, computations based on electron-impact ionization agree very well with the experiments. For other species, such as argon, tunneling-excitation should also be considered (see, e.g., V.L. Bastos de Jesus *et al*, to be published).
 - [24] This only holds if the interaction by which the first electrons dislodge the second is of contact type, i.e. $V_{12} = \delta(\mathbf{r}_1)\delta(\mathbf{r}_2 - \mathbf{r}_1)$. This interaction is implicit in Eq. (7). For other types of interactions see, e.g., Ref.[17].
 - [25] The start and return times coalesce at the maximal and minimal classically allowed momenta, defining a confined

region in phase space.

- [26] Longer excursion times are not relevant due to wave-packet spreading: the overlap between the wave packets of the first and of the second electron would be negligible. In our classical model, this implies leaving the corresponding electrons out of the ensemble.

- [27] Other sets of electrons ($t_0 \lesssim 1.5T$) do not contribute to the yield, since the corresponding tunneling rate is very small. Their influence is seen if this rate is artificially taken to be constant (c.f. lower panels of Fig.1).